# Supplementary Information:

# Tuning transport across $MoS_2$/graphene interfaces *via* as-grown lateral heterostructures

Shruti Subramanian[1,2], Ke Xu[3], Yuanxi Wang[4], Simon Moser[5,6], Nicholas A. Simonson[1,2], Donna Deng[1,2], Vincent H. Crespi[4], Susan K. Fullerton-Shirey[3,7], Joshua A. Robinson[1,2,8,9,*]

1. Department of Materials Science and Engineering, The Pennsylvania State University, University Park, Pennsylvania 16802, United States of America
2. Center for 2-Dimensional and Layered Materials, The Pennsylvania State University, University Park, Pennsylavnia 16802, United States of America
3. Department of Chemical and Petroleum Engineering, University of Pittsburgh, Pittsburgh, Pennsylavnia 15260, United States of America
4. Department of Physics, The Pennsylvania State University, University Park, Pennsylavania 16802, United States of America
5. Advanced Light Source, E. O. Lawrence Berkeley National Laboratory, Berkeley, California 94720, United States of America
6. Physikalisches Institut, Universität Würzburg, D-97074 Würzburg, Germany
7. Department of Electrical and Computer Engineering, University of Pittsburgh, Pittsburgh, Pennsylvania 15260, United States of America
8. 2-Dimensional Crystal Consortium, The Pennsylvania State University, University Park, Pennsylavania 16802, United States of America
9. Center for Atomically Thin Multifunctional Coatings, The Pennsylvania State University, University Park, Pennsylvania 16802, United States of America

## Supplementary Discussion

Gate tunability is critically important for optical and chemical sensing applications that require controllable charge separation. EG/$MoS_2$ interface properties leads to the lowest contact resistance, sheet resistance, and subthreshold slope, and highest on current demonstrating that EG is a better Ohmic contact compared to conventional metals. But the gate tunability offered by the EG/$MoS_2$ interface is significantly less than QFEG/$MoS_2$ due to the reduced Schottky barrier (and space charge region). Therefore, while QFEG may not be as improved a contact to $MoS_2$ as EG, it offers the maximum range of tunability compared to EG or metals due to a tunable energy barrier. In this form, QFEG/$MoS_2$ is a superior choice for tunable junction applications.

## Supplementary Note 1

The cross-sectional transmission electron micrograph (TEM) below shows that the interface between the epitaxial graphene (EG) and molybdenum disulfide ($MoS_2$) is in fact a pristine overlap at the interface.[1] $SiO_x$ is created by oxidation of the top few layers of the 6H SiC substrate during

the patterning of EG as explained in the main text. The $MoS_2$ nucleates at the edge of the EG and grows out onto the oxidized SiC and overlaps a little onto the EG on the other side. We do not have a precise control on the extent of overlap and have observed an overlap of 50-200 nm which helps in the electronic coupling of the EG with the $MoS_2$.

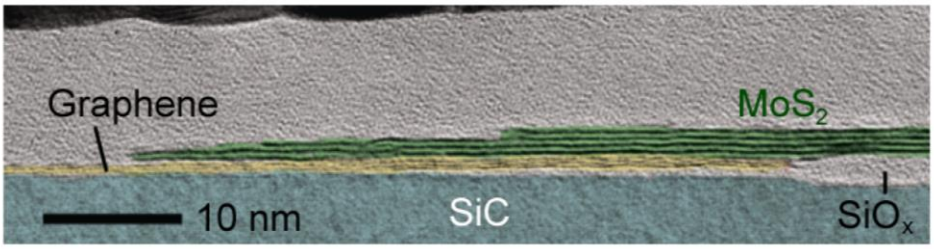


**Supplementary Figure 1:** Cross-sectional transmission electron micrograph (TEM) taken to show the pristine overlap at the interface of the epitaxial graphene (EG) and the molybdenum disulfide ($MoS_2$). This image was published in Carbon N. Y. **125,** Subramanian, S., Deng, D. D., Xu, K., Simonson, N., Wang, K., Zhang, K., Li, J., Feenstra, R., Fullerton-Shirey, S.K., Robinson, J. A., Properties of synthetic Epitaxial Graphene/Molybdenum Disulfide Lateral Heterostructures., 551–556, Copyright Elsevier (2017).[1]

## Supplementary Note 2

The contact resistance ($R_c$) and sheet resistance ($R_s$) is extracted for three structures – QFEG/$MoS_2$, EG/$MoS_2$ and metal/$MoS_2$. The values of $R_c$ and $R_s$ for the two heterostructures have been compared in the main text. Here, we show the values with respect to a conventional metal contact like Ti/Au. It is evident from Supplementary Figure 2 that both QFEG and EG provide to be improved contacts, but it is only the QFEG/$MoS_2$ case which allows for the modulation in values due to the unique p-n junction formation.

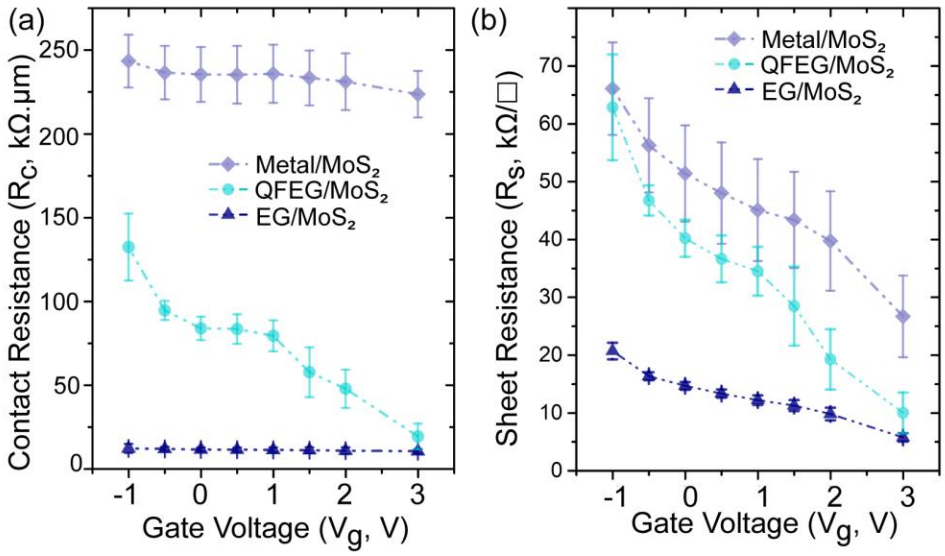


**Supplementary Figure 2:** (a) Contact resistance ($R_c$, kΩ•μm) versus Gate Voltage ($V_g$, V) - values extracted using transfer length method for QFEG/$MoS_2$, EG/$MoS_2$ and metal/$MoS_2$. Both QFEG and EG show an improvement in

contact resistance by over 20× at a $V_g$ value of +3V. (b) Sheet resistance ($R_s$, kΩ/• ) also shows the same characteristic trend for both the QFEG/$MoS_2$ and the EG/$MoS_2$ heterostructures, as compared to the metal/$MoS_2$ structures.

Supplementary Figure 3 shows the zoomed in dataset showing that upon application of gate voltage. Contact resistance with EG contacts is also tunable, but significantly lesser than the case of QFEG contacts. This in fact speaks to the novelty of this paper where we claim that EG is a better contact compared to QFEG (which is a better contact compared to conventional metals), but lacks the extent of gate tunability offered by QFEG due to the relative band alignments as shown *via* the μ-ARPES in Figure 3 of the main manuscript.

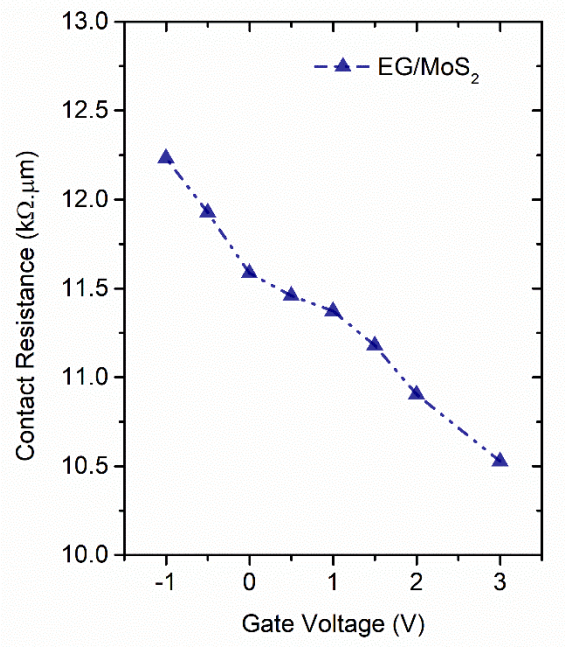


**Supplementary Figure 3:** Contact resistance ($R_c$, kΩ•μm) versus Gate Voltage ($V_g$, V) - values extracted using transfer length measurements for EG/$MoS_2$ heterostructure system. This is the zoomed in scale from Figure 2(a) of the main manuscript, denoting that the both EG/$MoS_2$ and QFEG/$MoS_2$ are gate tunable. QFEG/$MoS_2$ exhibits a significantly larger tunability due to the relative band alignments (shown in Figure 3 of the main manuscript) and larger space charge region of the synthesized p-n junction.

## Supplementary Note 3

The improved $R_c$ is accompanied by superior FET performance. A side gate geometry is employed as shown by the schematic in the inset of Figure 2(a) in the main text. In the case of EG (QFEG) contacts to $MoS_2$, the electrolyte gate modulates both the $MoS_2$ channel and the graphene contacts to the channel. For the sake of simplicity, an Au/Ti/$MoS_2$/Ti/Au system is represented by Metal/$MoS_2$, and an Au/Ti/EG(QFEG)/$MoS_2$/EG(QFEG)/Ti/Au system is represented as EG(QFEG)/$MoS_2$ in the text and legends of Figure 2 in the main text and Supplementary Figure 4 below. As evident from Supplementary Figure 4, the subthreshold slope *SS* for the Schottky barrier FETs[2] reduces from 312 to 216 to 89 mV/dec for $MoS_2$ contacted by Ti/Au, QFEG and EG, respectively. This represents a 70% and 30% improvement in SS for EG and QFEG, respectively, compared to typical Ti/Au contacts to $MoS_2$.

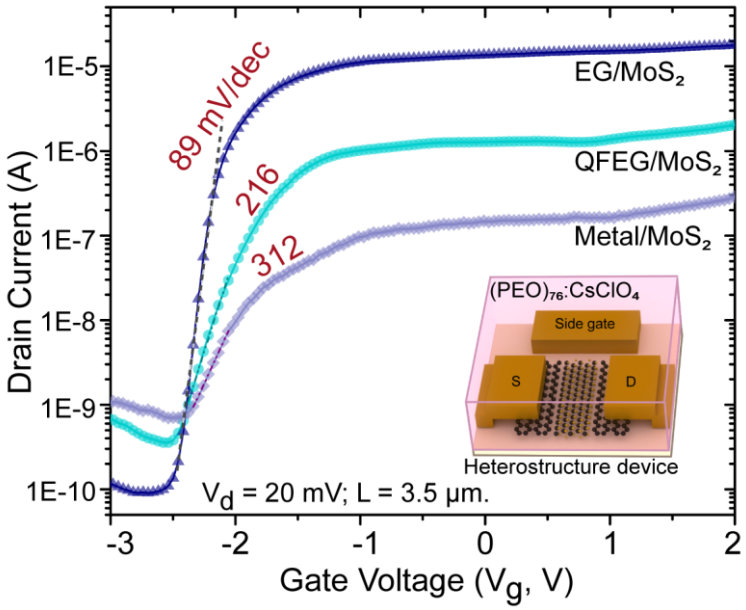


**Supplementary Figure 4:** Transfer curves displaying the same trend in subthreshold slope ($SS$) values as contact resistance data (i.e., EG/$MoS_2$ heterostructure has the smallest value of SS and $MoS_2$ contacted by Ti/Au has the maximum value of SS) in Figure S.2. On-currents ($I_{on}$) are also improved for EG/$MoS_2$ heterostructures due to reduced $R_c$ values. Inset shows a schematic of the side gate geometry employed for these measurements.

Subthreshold slope is a strong function of the ohmic contact energy barrier, and the superior subthreshold slope for the EG/$MoS_2$ device is attributed to the reduced Schottky barrier at the EG and $MoS_2$ interface. The Schottky barrier changes as a function of gate voltage ($V_g$) until the device turns *on* at $V_g$ > -1V. The trend is observed in comparison with the QFEG/$MoS_2$ and the metal/$MoS_2$ transfer curves. EG/$MoS_2$ has the steepest switching (lowest value of subthreshold slope – 89 mV/dec) as compared to QFEG/$MoS_2$ (216 mV/dec) and metal/$MoS_2$ (312 mV/dec). This trend is consistent with the band alignment and Schottky barrier at the interfaces – EG/$MoS_2$ has the smallest Schottky barrier followed by QFEG/$MoS_2$ and metal/$MoS_2$. The on current ($I_{on}$) is in the contact limited transistor performance regime, so the device with the lowest contact resistance has the highest $I_{on}$ after the device has turned *on*. Hence, EG/$MoS_2$ displays the highest magnitude of $I_{on}$ followed by QFEG/$MoS_2$ which has a 10× reduction compared to the EG/$MoS_2$, followed by metal/$MoS_2$ which has a 100× reduction when compared to the EG/$MoS_2$.

It is to be noted that off-current ($I_{off}$) has the opposite trend as compared to $I_{on}$. $MoS_2$/EG has the lowest $I_{off}$ followed by $MoS_2$/QFEG and then $MoS_2$/Ti/Au. This may lead to the conclusion of an improved $I_{on}/I_{off}$. However, when the applied $V_g$ is < -1V i.e. the device is *off*, we hypothesize that there is still a possible leakage path between the source and drain through the electrolyte with < 1 nA of current. Specifically, at negative voltages, where the device is *off*, anions accumulate near the channel, possibly forming a weakly conductive path from the source to drain, as shown *via* the dark grey arrows in Supplementary Figure 5. Thus, conclusive statements on the $I_{on}/I_{off}$

ratios cannot be made. It is important to point out that this *off* current is of the order of < 1 nA, which is more than 4 orders of magnitude smaller than the current of the channel when the transistor is switched on (>10 μA) – hence, the potential presence of such a path does not impact our conclusions of $R_c$ as it is derived from $V_g$ > -1V and the channel current is ≥ 0.1 μA.

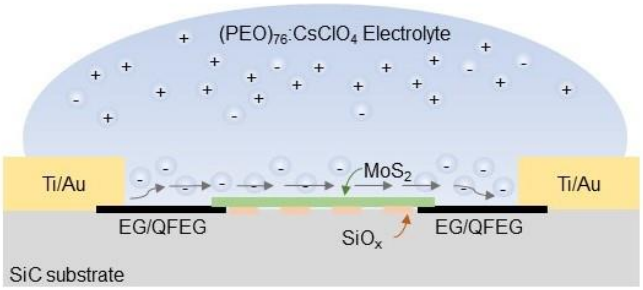


**Supplementary Figure 5:** A cross-sectional schematic of the heterostructure devices showing the Ti/Au contact and the $(PEO)_{76}$:$CsClO_4$ solid polymer electrolyte on top. Upon application of a negative side gate voltage, anions drift to the electrolyte/2D channel interface forming an electric double layer (EDL). The side gate (not included in this schematic) is where the cationic double layer is located.

Also, it is to be noted that the value of the *off* current will likely depend on the type of charge carriers in the graphene/$MoS_2$ system because the number of ions forming the conduction path will change in each system. For example, EG is *n*-doped and has electrons as carriers, which will repel the negatively charged anions in the electrolyte possibly leading to the smaller leakage current and smaller total $I_{off}$ between the source and drain. QFEG on the other hand, is *p*-doped and hence, attracts more anions than the EG, leading to a stronger conduction path between the source and drain within the electrolyte, and hence, a larger total value of $I_{off}$. For the case of $MoS_2$ directly contacting metal (i.e., without the addition of graphene), the distance between source and drain metal is the shortest (3.5 μm compared with 13.5 μm with graphene). This may lead to a larger value of $I_{off}$.

Notice that the explanation offered above is speculative based on what we know about the formation of EDLs at the channel interface. Therefore, conclusive statements about the impact of using a graphene contact to $MoS_2$ in terms of $I_{on}/I_{off}$ ratios and their trends between systems cannot be made. Prior to the electrolyte gate measurement of at least four TLM sets of both the heterostructure and the $MoS_2$-only devices, it is essential to establish a voltage sweep rate which would minimize the hysteresis while taking the measurements at a reasonable rate as well. Supplementary Figure 6 shows the forward and reverse sweeps for different voltage sweep rates indicating that there is a good repeatability of the data within the same direction of sweep. The hysteresis has not been eliminated but minimized while maintaining a reasonable time for the measurements, and the sweep rate thus established has been maintained constant throughout the experiments. This has been repeated for several channel lengths with very similar results. Note

that the direction of the hysteresis in the double sweeps is counter-clockwise, which is commonly observed in EDL-gated FETs.[3–6]

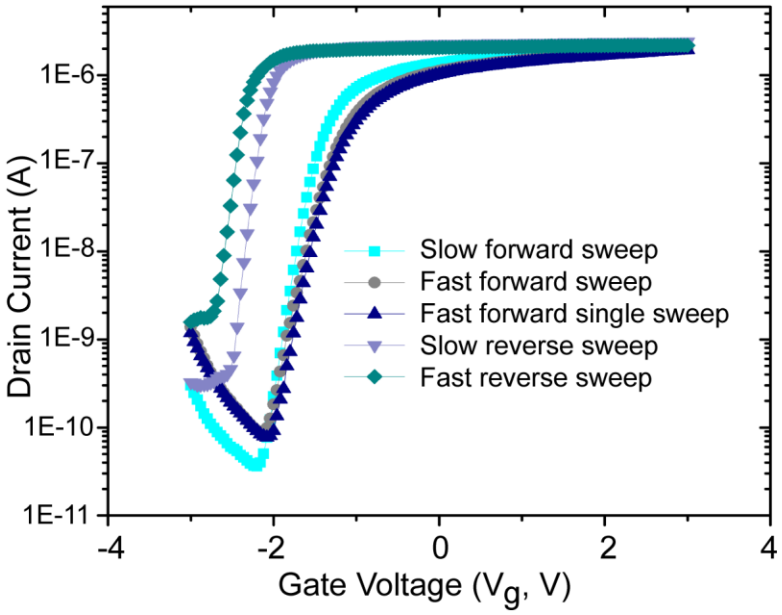


**Supplementary Figure 6:** Transfer curves for a 3.5 µm channel in an EG/$MoS_2$/EG heterostructure system. The forward and reverse sweeps refer to the direction of the voltage sweep and the slow (0.67 mV/s) and fast (3 mV/s) refer to the sweep rate.

## Supplementary Note 4

Work functions of EG and QFEG have been calculated from first-principles previously and are summarized below. For EG, DFT calculations reported a Fermi level 0.4 eV above the Dirac point[7], yielding a $4.55 - 0.4 = 4.15$ eV work function, consistent with the experimentally reported $\phi_{EG} = -4.2$ eV used in the main text.

For QFEG, the Fermi level shift is more challenging to model from DFT since the doping originates from a surface charge (due to the bulk polarization of 6H-SiC)[8,9], instead of from the dangling bonds at the graphene/SiC interface. The electrostatic energy associated with these uncompensated charges at polar surfaces are not large enough to trigger charge redistribution when conventional few-layer SiC slab geometries are used in DFT calculations, with Si- and C-terminations (both fully passivated by hydrogen), and would result in an incorrect Fermi level coinciding with the Dirac point. Supplementary Reference 2 shows that even the SiC polytype with the largest polarization, 2H-SiC, only results in a potential drop of ~2 eV across a slab of 12 SiC repeating units along the *z* direction (perpendicular to the 0001 surface), i.e. still smaller than the 2H-SiC bulk band gap so that charge transfer from graphene to the SiC conduction band would not occur[8]. Thus, a model using 6H-SiC, with a bulk polarization smaller than the 2H polytype, would require hundreds of repeating SiC units before charge compensation can occur. In

Supplementary Reference 2, this was circumvented by passivating the C-terminated SiC surface with bilayer Au, which serves as a computational device to provide mid-gap metallic states capable of redistributing charge between graphene and itself[8]. With this method and alternative Green's function methods, Supplementary Reference 2 reports a downward Fermi level shift of 0.18 eV from the Dirac point, yielding a work function of $4.55 + 0.18 = 4.73$ eV, consistent with $\phi_{QFEG} = -4.7$ eV used in the main text.

## Supplementary Note 5

Cross sectional transmission electron microscopy reveals that the $MoS_2$ channel is predominantly bilayer, which supports the value of bandgap for $MoS_2$ used for the theoretical reconstruction of the band structure of the lateral $MoS_2$/EG(or QFEG) heterostructure interface.

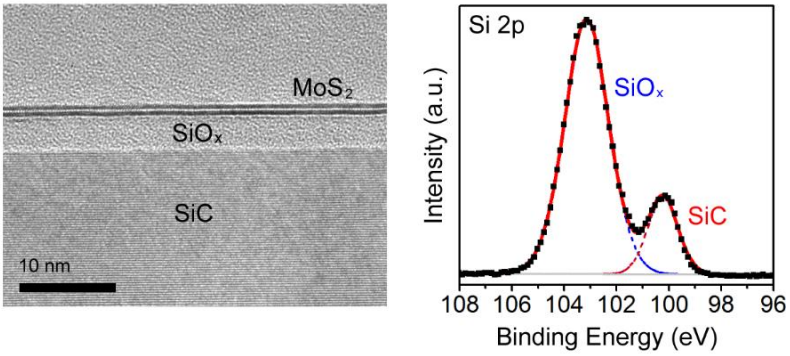


**Supplementary Figure 7:** Cross sectional transmission electron micrograph shows bilayer $MoS_2$ in the channel, away from the interface with the graphene. X-ray photoelectron spectroscopy (XPS) shows the presence of an oxide of Silicon which is present underneath the $MoS_2$, as seen from the cross-sectional TEM.

## Supplementary References


1. Subramanian, S. *et al.* Properties of synthetic epitaxial graphene/molybdenum disulfide lateral heterostructures. *Carbon N. Y.* **125**, 551–556 (2017).

2. Appenzeller, J. *et al.* Toward Nanowire Electronics. *IEEE Trans. Electron Devices* **55**, 2827–2845 (2008).

3. Pu, J. *et al.* Highly flexible $MoS_2$ thin-film transistors with ion gel dielectrics. *Nano Lett.* **12**, 4013–4017 (2012).

4. Pu, J. *et al.* Fabrication of stretchable $MoS_2$ thin-film transistors using elastic ion-gel gate dielectrics. *Appl. Phys. Lett.* **103**, 023505 (2013).

5. Xu, H., Fathipour, S., Kinder, E. W., Seabaugh, A. C. & Fullerton-Shirey, S. K. Reconfigurable Ion Gating of 2H-$MoTe_2$ Field-Effect Transistors Using Poly(ethylene oxide)-$CsClO_4$ Solid Polymer Electrolyte. *ACS Nano* **9**, 4900–4910 (2015).

6. Fujimoto, T., Miyoshi, Y., Matsushita, M. M. & Awaga, K. A complementary organic inverter of porphyrazine thin films: low-voltage operation using ionic liquid gate dielectrics. *Chem. Commun.* **47**, 5837 (2011).

7. Mattausch, A. & Pankratov, O. Ab initio study of graphene on SiC. *Phys. Rev. Lett.* **99**, 1–4 (2007).

8. Sławińska, J., Aramberri, H., Muñoz, M. C. & Cerdá, J. I. Ab initio study of the relationship between spontaneous polarization and p-type doping in quasi-freestanding graphene on H-passivated SiC surfaces. *Carbon N. Y.* **93**, 88–104 (2015).

9. Ristein, J., Mammadov, S. & Seyller, T. Origin of Doping in Quasi-Free-Standing Graphene on Silicon Carbide. *Phys. Rev. Lett.* **108**, 246104 (2012).